

QUASI P_1^0 ELECTROMAGNETIC RESPONSE ESTIMATES FROM ØRSTED VECTOR DATA: A STUDY IN RING CURRENT ASYMMETRY

Nicola C. Richmond⁽¹⁾, Catherine G. Constable⁽²⁾, Steven Constable⁽³⁾, Joseph Ribaudo⁽⁴⁾

IGPP, Scripps Institution of Oceanography, University of California, La Jolla, 92093-0225, USA
Email: ⁽¹⁾ nic@ucsd.edu, ⁽²⁾ cconstable@ucsd.edu, ⁽³⁾ sconstable@ucsd.edu, ⁽⁴⁾ jribaudo@ucsd.edu

ABSTRACT

Previous studies have shown that mantle electrical conductivity profiles can be derived from satellite magnetometer data. The approach uses available field models (e.g. CHAOS, CM4) to remove unwanted magnetic sources, in order to isolate external variations due to the magnetospheric ring current and associated induced currents within the Earth. Here, we report progress evaluating vector Ørsted data on a pass-by-pass basis. Between approximately 2am and 10am local time, a satellite estimate of ring current intensity (SatDst) consistently underestimates the magnitude of the geomagnetic index SYM-H; the difference is larger the more negative SYM-H. In contrast, between approximately 2pm and 10pm local time, SatDst gives values with larger magnitude than SYM-H; typically these are more negative values. This indicates that we are observing asymmetry in the source field, possibly due to the partial ring current. Our estimates of frequency dependent response functions for hourly local time bins show the influence of this source current asymmetry. A preliminary electrical conductivity profile for one local time suggests the presence of a conductivity jump in the lower mantle.

1. INTRODUCTION

Understanding the electrical conductivity of Earth's interior has the potential to provide information on the composition, temperature, pressure, and minor element distribution in the mantle. Electrical conductivity profiles can be derived by studying currents induced within the Earth by external, time-varying magnetic fields associated with ionospheric or magnetospheric current systems. Many studies have used observatory data [e.g. 1], but it has been shown [2, 3] that satellite data can also be used. In this case, the source current of interest is the magnetospheric ring current, a toroidal current circling Earth in the geomagnetic equatorial region at 2-9 Earth radii (Fig. 1). Two geomagnetic indices describe the intensity of the ring current: the hourly Dst index and 1-minute SYM-H index.

A previous induction study using Magsat vector data [4] found evidence for a conductivity jump at $\sim 1,300$ km. This depth is below the transition zone and does not correspond to any currently known mineral transition or phase change. However, the depth that can be sampled by electromagnetic induction techniques is dependent on the length of the time series available. Magsat

provided 7 months of data and 1,300 km is close to the depth resolution of those data. Consequently, the existence of a lower mantle conductivity jump is uncertain based on those data alone. Other work has also indicated the possibility of a conductivity jump in the lower mantle [5], but at a depth of 900 km rather than 1,300 km. In contrast, other recent studies have found no evidence of a lower mantle conductivity jump [6].

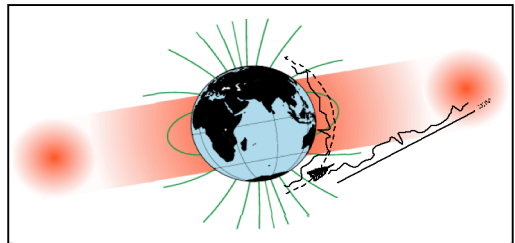


Figure 1. The magnetospheric ring current.

Here, we report the results of a study using vector Ørsted satellite data from November 2000 to December 2005. Residuals from field models are used to isolate the internal and external field contributions associated with the magnetospheric ring current. The results have been used to calculate a satellite estimate of ring current activity (SatDst) and frequency dependent response functions. Ørsted drifts slowly in local time (LT), by about 1 hour every 2 months. Hence we have at least 2 sets of coverage for all LTs. We report a comparison between SatDst and SYM-H as a function of LT and year, and the associated effects of LT on response function estimation. A preliminary electrical conductivity profile is presented and discussed for a single local time.

2. DATA PROCESSING

The magnetospheric ring current and the associated induced currents within the Earth have been isolated by using available field models to remove unwanted field components. In this study, we have used CHAOS [7] to remove the core field and its secular variation, and CM4 [8] to remove the lithospheric, ionospheric, constant magnetospheric and toroidal fields.

In geomagnetic coordinates aligned with the internal dipole axis, the ring current has predominantly P_1^0 structure at mid-latitudes [9]:

$$\Phi_1^0(r, \theta) = a_0 \left\{ i_1^0(t) \left(\frac{a_0}{r} \right)^2 + e_1^0(t) \left(\frac{r}{a_0} \right) \right\} P_1^0(\cos \theta) \quad (1)$$

The magnetic induction B is derived from the negative of the gradient, which is given by Eqs 2-4 (as components of a spherical coordinate system).

$$B_r = \left[-e_1^0 + 2i_1^0 \left(\frac{a}{r} \right)^3 \right] \cos(\theta) \quad (2)$$

$$B_\theta = \left[e_1^0 + i_1^0 \left(\frac{a}{r} \right)^3 \right] \sin(\theta) \quad (3)$$

$$B_\phi = 0 \quad (4)$$

After removing unwanted components using CHAOS and CM4, e_1^0 and i_1^0 have been estimated for each satellite pass using an overdetermined least squares approach. A satellite estimate of ring current activity can then be estimated for each pass using Eq. 5:

$$SatDst = e_1^0 + i_1^0 \quad (5)$$

3. SATDST ESTIMATES AS A FUNCTION OF LOCAL TIME

For the Ørsted data from November 2000 to December 2005, we have estimated e_1^0 , i_1^0 and SatDst using the method described in section 2. Consistent with previous studies [4, 10], we find that i_1^0 is equal to approximately $0.3 e_1^0$.

Fig. 2 presents a comparison between SatDst and pass-

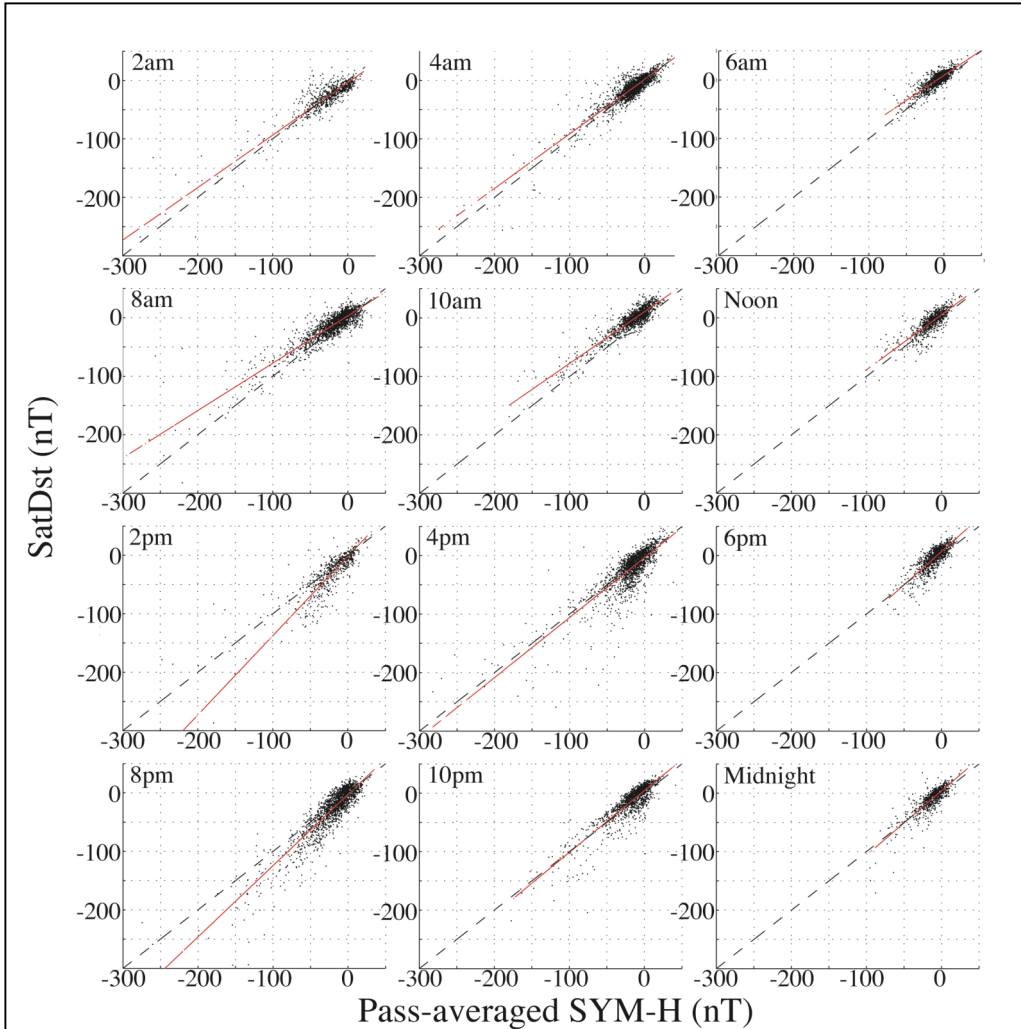


Figure 2. Scatterplots of SatDst against pass-averaged SYM-H for 12 one-hour local time bins, plotted using a fixed range of -300 to 50 nT for comparison. The black dotted line shows a 1-to-1 relationship, while the red line gives the best fit to the data.

averaged values of the SYM-H geomagnetic index [11] as a function of local time, for the full time series used in this study. For a symmetric ring current, it would be expected that the SatDst estimates for each local time would have an approximately 1-to-1 relationship with SYM-H (black dotted line in Fig. 2). However, we find a systematic difference between SatDst and SYM-H as a function of local time. Between ~2am and 10am, SatDst underestimates the magnitude of SYM-H and the difference is larger, the more negative SYM-H. However, for local times between ~2pm and 10pm, SatDst consistently overestimates the magnitude of SYM-H and again the difference is larger the more negative SYM-H. These observations are consistent with an asymmetry in the source field.

It is likely that one of the causes of the observed asymmetry is the partial ring current [e.g. 12]. This current results from the injection of particles into the inner magnetosphere from the geomagnetic tail during magnetic storms. The injected particles drift westwards through dusk before closing via the magnetopause or auroral currents at local times close to noon. This would result in a stronger external field between noon and midnight (via dusk) and a weaker external field during the hours near dawn. The results in Fig. 2 are consistent with this.

There are other factors that could be contributing to the observed asymmetry, including ionospheric fields and other magnetospheric sources. We use CM4 to correct for ionospheric currents, but the power spectra of the dayside internal coefficients indicate that those data are still contaminated by frequencies associated with the Sq ionospheric sources. The cross-tail current in the magnetosphere may also be contributing to the differences we are seeing.

4. LONG PERIOD CHANGES TO THE ASYMMETRY?

Fig. 3 compares the gradient of the best-fit lines between SatDst and pass-averaged SYM-H as a function of local time. The best-fit lines have been determined separately for each year of data, rather than for the compilation of years shown in Fig. 2.

The gradient is steeper for some years than others (e.g. 2001 and 2003 for local times between 3 and 6 hours) indicating that the difference between SatDst and pass-averaged SYM-H is larger in some years than others. In some years, the relationship between SatDst and SYM-H is not as well constrained as other years due to limited coverage for a given year. Additionally, the best-fit line is strongly dependent on storm time estimates of SatDst but for some LTs during some years there were fewer storm events than at other times. However, even taking these factors into account, the relationship between SatDst and SYM-H appears to be slightly different in different years. The reason for this is uncertain. It may

be related to the solar cycle, but the current lack of available data for the full solar cycle means this cannot be verified.

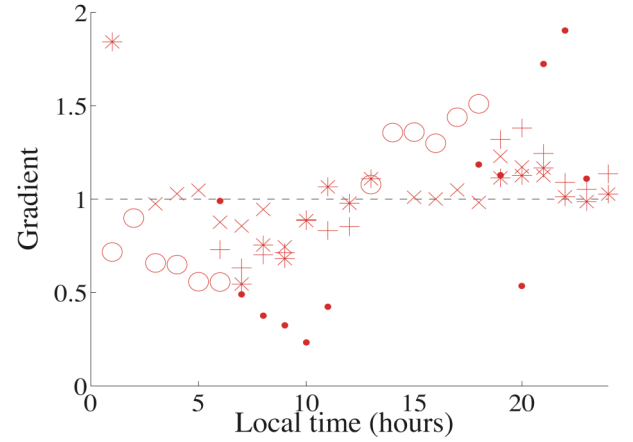


Figure 3. Gradient of the best-fit line between SatDst and pass-averaged SYM-H as a function of local time and year. \times 2001; $+$ 2002; \circ 2003; $*$ 2004; \bullet 2005.

5. LOCAL TIME EFFECTS ON RESPONSE FUNCTION ESTIMATES

Considering only conductivity variations as a function of radius within the Earth, the external field variations will induce internal fields with P_1^0 structure and a magnitude which depends on Earth conductivity. Thus, the frequency dependent transfer function Q (Eq. 6) can be used to infer the conductivity structure of the Earth. We used multitaper cross-spectral estimation [13] with 20 tapers to estimate Q . The complex admittance function C [14] was then calculated using Eq. 7, where a is the radius of the Earth and l is the order of the spherical harmonic function used to estimate Q , in this case 1.

$$Q_l(f) = \frac{i_l(f)}{e_l(f)} \quad (6)$$

$$C = a \frac{l - (l+1)Q_l}{l(l+1)(1+Q_l)} \quad (7)$$

Fig. 4 presents the real (+) and imaginary (\circ) parts of C for different local time bins from 2001-2003. The coherency cutoff for the data in Fig. 4 is either 0.6 or 0.8. Where possible 0.8 was used, but in order to provide improved coverage, 0.6 was used in two cases. For 12-16 hrs, there was a large gap in the data and therefore only short periods have been studied. Nightside data give values close to those of [15]. Dayside values, particularly for the real component, are quite different to the nightside data. The differences

among the data sets in Fig. 4 are caused by local time effects in the source current. Although these differences diminish at longer periods (as predicted by [15]), the data do not fully converge.

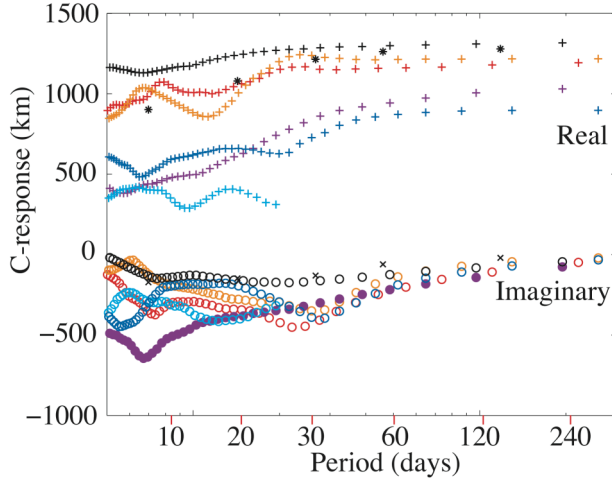


Figure 4. C estimates for different local times. Magsat values from (4) are shown in black (* and ×) for comparison.

Red	0-4 hrs	2003 (coherency > 0.6)
Orange	4-8 hrs	2001 (coherency > 0.8)
Purple	8-12 hrs	2002 (coherency > 0.8)
Cyan	12-16 hrs	2003 (coherency > 0.8)
Blue	16-20 hrs	2001 (coherency > 0.6)
Black	20-24 hrs	2002 (coherency > 0.8)

It is noted that Magsat C estimates from [4] were determined using dusk data. Comparison with equivalent Ørsted data (LTs 16-20 hours shown in blue in Fig. 4) indicates there is a large difference between the Magsat and Ørsted dusk data. Indeed, the Magsat data provides C values that are much closer to the nightside Ørsted values. It is possible that this difference is due to different toroidal fields at the satellite altitudes (325-550 km for Magsat and 500-850 km for Ørsted). While we use CM4 to correct for toroidal fields in the processing of the Ørsted data, current understanding of these fields is limited and it is likely that the data presented here are still affected by toroidal fields. CHAMP is orbiting at an altitude closer to that of Magsat. Estimates of C at dusk for that satellite would indicate whether altitude effects are a factor in the differences between the Magsat and Ørsted dusk data.

6. ELECTRICAL CONDUCTIVITY ESTIMATES

The response functions in Fig. 4 have been used to estimate 1-D mantle electrical conductivity profiles. Prior to inversion the response estimates are averaged in frequency bins that are approximately logarithmically spaced to reflect the available frequency resolution in the estimates. The uncertainties produced in this process are almost certainly unrealistically low, so they have

been boosted to 50 km to reflect likely departures from 1D mantle structure and data covariance within the frequency bins. A preliminary result is presented in Fig. 5A for local times from 4-8 hours (orange data from Fig. 4). The profile was determined using the OCCAM method [16] with an RMS misfit of 2.0. A comparison of predictions from the model and the data is given in Fig. 5B.

It is notable that the preliminary conductivity profile in Fig. 5A supports a conductivity increase at $\sim 1,300$ km, supporting the earlier result of [4]. This depth does not correspond to any known seismic discontinuity and it has not been identified as a depth corresponding to a mineralogical phase transition. It has been suggested that there may be a change in the way in which aluminum incorporates into perovskite in the upper part of the lower mantle [e.g. 17] and [18, 19] have shown that aluminum could increase the incorporation of ferric iron into perovskite. This could potentially have a role in the observed increase in conductivity shown in Fig. 5A. However, further work is needed to confirm the existence of the lower mantle conductivity jump.

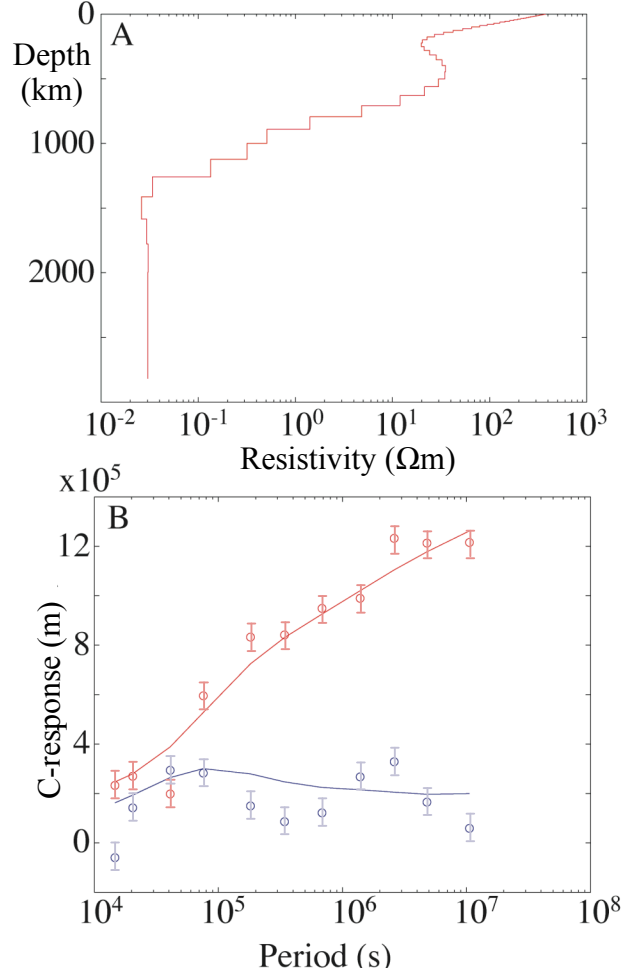


Figure 5. A: 1-D electrical conductivity profile for LT 4-8 hours. B: Comparison of data (circles) and model (lines) for the real (red) and imaginary (blue) parts of C for 4-8 hours.

The conductivity profile reported here is a preliminary result for one 4-hour LT range. Given that the C-responses depend quite strongly on LT, it will be necessary to estimate 1-D conductivity profiles for all local times to study the impact on mantle conductivity estimates. However, it is noted that the key aspect of the C-response that influences estimates of lower mantle conductivity is the long period imaginary component. It is clear in Fig. 4 that, while there are differences among local times, the long period imaginary components are very similar for all LTs. In addition, while this study has identified differences between dusk C-responses for Magsat and Ørsted, these are only in the real component, not the imaginary. Consequently, it seems likely that neither the LT nor altitude effects will affect the study of lower mantle conductivity by satellite induction studies using the method reported here.

7. SUMMARY

Using over 5 years of Ørsted data, we have obtained estimates of the internal and external fields associated with the magnetospheric ring current, as a function of LT and year. The results have shown clear LT asymmetry in the source current, potentially due to the partial ring current. The effect of the LT asymmetry in the estimation of frequency dependent response functions indicate that dayside C estimates differ considerably from nightside values. However, the imaginary component of C at long periods, which is important in estimates of lower mantle conductivity, is similar for all LTs. A preliminary 1-D conductivity profile supports the existence of a conductivity jump at ~1,300km.

8. REFERENCES

1. Olsen N., *Geophys. J. Int.*, 138, 179-187, 1999.
2. Dolginov, *Geomag. Aeron.*, 12, 611-617, 1972.
3. Olsen N., *Surv. Geophys.*, 20, 309-340, 1999.
4. Constable S. and Constable C., *G³*, 5, doi:10.1029/2003GC000634, 2004.
5. Everett M., 1st Swarm International Science Meeting, Nantes, France, 2006.
6. Kuvshinov A., 1st Swarm International Science Meeting, Nantes, France, 2006.
7. Olsen N. et al., *Geophys. J. Int.*, in press, 2006.
8. Sabaka T. et al., *Geophys. J. Int.*, 159, 521-547, 2004.
9. Banks R., *Geophys. J. R. Astron. Soc.*, 17, 457-487, 1969.
10. Langel R. and Estes R., *J. Geophys. Res.*, 90, 2487-2494, 1985.
11. Available from:
<http://swdcwww.kugi.kyoto-u.ac.jp/wdc/Sec3.html>
12. Liemohn M. et al., *J. Geophys. Res.*, 106, 10,883-10,904, 2001.
13. Riedel K. and Sidorenko A., *IEEE Trans. Signal Process.*, 43, 188-195, 1995.
14. Weidelt P., *Zeit. Geophys.*, 38, 257-289, 1972.
15. Balasis G. et al., *Geophys. Res. Lett.*, doi:10.1029/2004GL020147, 2004.
16. Constable S. et al., *Geophys.*, 52, 289-300, 1987.
17. Brodholt J. P., *Nature*, 407, 620-622, 2000.
18. Wood B. J. and Rubie D. C., *Science*, 273, 1522-1524, 1996.
19. Richmond N. C. and Brodholt J. P., *Am. Min.*, 83, 947-951, 1998.